JOURNAL OF NEUROTRAUMA 31:268–283 (February 1, 2014)

DOI: 10.1089/neu.2013.3108

The Cancer Drug Tamoxifen: A Potential Therapeutic Treatment for Spinal Cord Injury

Jutatip Guptarak,[1] John E. Wiktorowicz,[1] Rovshan G. Sadygov,[1] Dragoslava Zivadinovic,[1] Adriana A. Paulucci-Holthauzen,[1] Leoncio Vergara,[2] and Olivera Nesic[1,3]

Abstract

Tamoxifen (TMX) is a selective estrogen receptor modulator that can mimic the neuroprotective effects of estrogen but lacks its systemic adverse effects. We found that TMX (1 mg/day) significantly improved the motor recovery of partially paralyzed hind limbs of male adult rats with thoracic spinal cord injury (SCI), thus indicating a translational potential for this cancer medication given its clinical safety and applicability and the lack of currently available treatments for SCI. To shed light on the mechanisms underlying the beneficial effects of TMX for SCI, we used proteomic analyses, Western blots and histological assays, which showed that TMX treatment spared mature oligodendrocytes/increased myelin levels and altered reactive astrocytes, including the upregulation of the water channels aquaporin 4 (AQP4), a novel finding. AQP4 increases in TMX-treated SCI rats were associated with smaller fluid-filled cavities with borders consisting of densely packed AQP4-expressing astrocytes that closely resemble the organization of normal glia limitans externa (in contrast to large cavities in control SCI rats that lacked glia limitans-like borders and contained reactive glial cells). Based on our findings, we propose that TMX is a promising candidate for the therapeutic treatment of SCI and a possible intervention for other neuropathological conditions associated with demyelination and AQP4 dysfunction.

Key words: AQP4; tamoxifen; myelin; proteomics; spinal cord injury

Introduction

A PROTECTIVE EFFECT of estrogen in the central nervous system (CNS) has been demonstrated in different neuropathological conditions,[1–4] including in spinal cord injury (SCI).[5] However, the therapeutic potential of exogenous estrogens is limited due to estrogen-induced peripheral feminizing and potentially dangerous proliferative effects. Therefore, selective estrogen receptor modulators such as tamoxifen (TMX)—which can specifically induce beneficial estrogenic mechanisms in the CNS but lack estrogen's systemic adverse effects—have a better therapeutic potential.

Estrogen receptors (ER) are expressed both in neurons and glia,[6] including astrocytes[7] and oligodendrocytes.[8] TMX and/or its metabolites bind to ERs and induce tissue-specific changes in their three-dimensional conformation,[9,10] allowing a tissue- and cell- selective recruitment of different transcriptional cofactors,[11–14] which explains why TMX acts as an ER agonist in the brain and an ER antagonist in others tissues (e.g., breast). In the CNS, TMX also can have diverse effects depending on the cell type, it can mimic estrogen's effects on oligodendrocytes[15] but can antagonize estrogens' effects on astrocytes.[16] Further, TMX can stimulate signaling pathways that are independent of ER activation.[17] For example, TMX inhibits protein kinase C in an estrogen-independent fashion in the brain, and because of this activity, is currently in clinical trials for bipolar disorder.[18] TMX also inhibits swelling-activating anion channels[19] in an ER-independent fashion, which is believed to contribute to its neuroprotective effects in brain ischemia.[20] Beneficial effects of TMX also have been demonstrated in such other neuropathological conditions as traumatic injury to the central and peripheral nervous system, stroke, multiple sclerosis, Parkinson's disease, Alzheimer's disease, cognitive decline, and mood disorders,[21] including SCI.[22,23]

Our goal in this study was to test the translational potential of TMX in a rat model of moderate contusion SCI, and to use proteomic, biochemical and histological analyses to shed light on the mechanisms underlying TMX's beneficial effects in injured spinal cords.

Methods

Contusion injury

Male Sprague-Dawley rats (Harlan, 225–250 g) were anesthetized with pentobarbital (50 mg/kg, intraperitoneal); our procedure

[1]Department of Biochemistry and Molecular Biology, [2]Center for Biomedical Engineering, University of Texas Medical Branch, Galveston, Texas.
[3]Department of Medical Education Texas Tech University Paul L. Foster School of Medicine, El Paso, Texas.

was detailed in an article by Durham-Lee and colleagues.[24] Animals were contused at the tenth thoracic segment (T10) with an Infinite Horizons Impactor using a force of 150 kdynes (1 sec dwell time). All procedures complied with the recommendations in the National Institutes of Health's *Guide for the Care and Use of Laboratory Animals* and were approved by the University of Texas Medical Branch (UTMB) Animal Care and Use Committee. Control age-matched animals were not subjected to any part of the surgical or post-surgical care protocols. We use only naïve rats as controls, as we discussed in Durham-Lee and colleagues.[24]

Tamoxifen treatment

Timed-release tamoxifen pellets (Innovative Research of America; Catalog #E-351) were surgically implanted subcutaneously (on the lateral side of the neck between the ear and shoulder) 2 h after SCI as a clinically relevant time for drug administration. Drug administration via pellets was advantageous because it significantly reduced the distress of animals versus prolonged daily intraperitoneal or intravenous injections; one of our goals was to test different durations of TMX delivery. In addition, subcutaneous pellets would have an advantage even for clinical applications. The TMX pellets were designed for a constant delivery rate of 1mg/day for 14 days or 28 days. Tamoxifen pellets have been used in several other animal studies (listed on the manufacturer's web site: http://www.innovrsrch.com/reference/searchResults2.asp). Using similar pellets, Kisanga and colleagues[25] demonstrated stable, consistent levels of serum TMX at different times after pellet implantation. One mg/day/rat dose is similar to the dose that has already shown neuroprotective effects in SCI.[23] This TMX dose is about 10 times higher than used in breast cancer patients but it is lower than TMX dose used in the experimental treatment of glioblastoma patients,[26] and thus it is clinically applicable.

Assessing possible adverse effects of tamoxifen. TMX can cause liver cancer in rats,[27] unlike in humans. Although TMX doses that can cause adverse effects in normal rats are 10 times higher than used in our study,[27] we assessed TMX's tumorigenic activity in SCI rats, since their drug metabolism is altered, and thus their susceptibility to drugs' adverse effects higher. Therefore, we weighed the livers in both groups of SCI rats (35 days after SCI), but we found no significant differences between groups. The average weights of livers in naïve ($n = 10$; standard deviation), control SCI, and TMX-treated SCI rats are in the table below. Further, gross histological assessments of liver and intestinal organs performed by a UTMB veterinarian showed no pathological alterations.

	MEAN (gram)	SD
Naïve	13.342	0.6279
SCI	12.485	0.7709
TMX	12.743	0.8343

Locomotor assessment

Hind-limb movement was assessed using the Basso, Beattie, and Bresnahan (BBB) Scale.[28] BBB scores were collected daily on the first 14 days after injury, and once weekly thereafter.

Protein extraction

Animals were anesthetized by intraperitoneal injection of pentobarbital (150 mg/kg) and sacrificed by transcardial perfusion with 0.9% saline containing heparin. T10 (lesion epicenter) and lumbar (L1-L5) spinal cord segments were removed and stored at −80°C. For protein extraction, we used ProteinExtract™ complete Mammalian Proteome Extraction Kits (Calbiochem Cat No. 539779). Protein concentrations were determined using the RC DC Protein Assay Kit (BioRad cat #500-0122).

Proteomic separations and analysis

Proteins were analyzed by two-dimensional gel electrophoresis as described previously.[29,30] See supplementary material for a detailed description.

Electrophoresis and Western blotting

As detailed by Guptarak and colleagues,[31] samples containing 40 (g of protein were mixed with an appropriate volume of 6× super-denaturing sample buffer and equal amounts of protein were loaded onto a sodium dodecyl sulfate-polyacrylamide gel; the samples were not boiled to avoid aggregation of membranous proteins.

Immunofluorescence

The method is detailed by Guptarak and colleagues.[31] Spinal cords were removed, postfixed overnight at 4°C in 4% paraformaldehyde, and cryoprotected in phosphate buffer with 30% sucrose for three days. The sections were washed in 0.05M TBS mounted on gelatin-coated glass slides, and dried before the addition of mounting medium with the nuclear stain 4',6-diamidino-2-phenylindole, dihydrochloride (DAPI; Vector Laboratories H-1200, Iowa City, IA).

Primary antibodies

Primary antibodies (Table 2) used were: mouse anti-CC1 (Abcam # ab16794 1:100, Cambridge, MA), a mature oligodendrocyte marker APC (or CC1) that is an antagonist of β-catenin and results in a reduction in Wnt signaling[32]; rabbit anti-aquaporin 4 (AQP4; Millipore/AB 3594 1:10,000, Billerica, MA); mouse anti-3CB2 (Hybridoma bank; 1:1000, Iowa City, IA), an intermediate filament-associated protein specifically expressed in embryonic radial glia[33]; and mouse anti-Iba-1 (Wako Pure Chemicals 1:1000, Osaka, Japan), an ionized calcium binding adaptor molecule 1 that is specifically expressed at low levels in resting microglia but at high levels in activated microglia/macrophages.

Image acquisition and analysis

Images were collected using a Zeiss LSM-510 META confocal microscope with a 10×0.3 numerical aperture (NA) lens and a 63× oil 1.4 NA objective (Optical Microscopy Core at UTMB). The images were obtained using excitation lines at 364, 488, and 543 nm and three different channels of emission with sequential acquisition. 3D rendering was done using Imaris Premier 7.5 software. See supplementary material for a more detailed description.

Statistical analysis

All statistical tests were evaluated at the α level of 0.05, with two-tailed *t*-test, using the SPSS program. For multiple-group comparisons, data were analyzed using analysis of variance. The LSD multiple comparisons *post-hoc* test was used to determine *p* values (< 0.05).

In all our graphs, ''#'' is used to denote significant difference ($p < 0.05$) between uninjured rats and control SCI rats and ''*'' to denote significant difference ($p < 0.05$) between control SCI rats and TMX-treated SCI rats.

To identify differentially expressed gel spots in the proteomic analyses we used *t*-tests to compare the ($\log^2$ transformed) intensity of spots. The comparisons were first made for uninjured versus SCI,

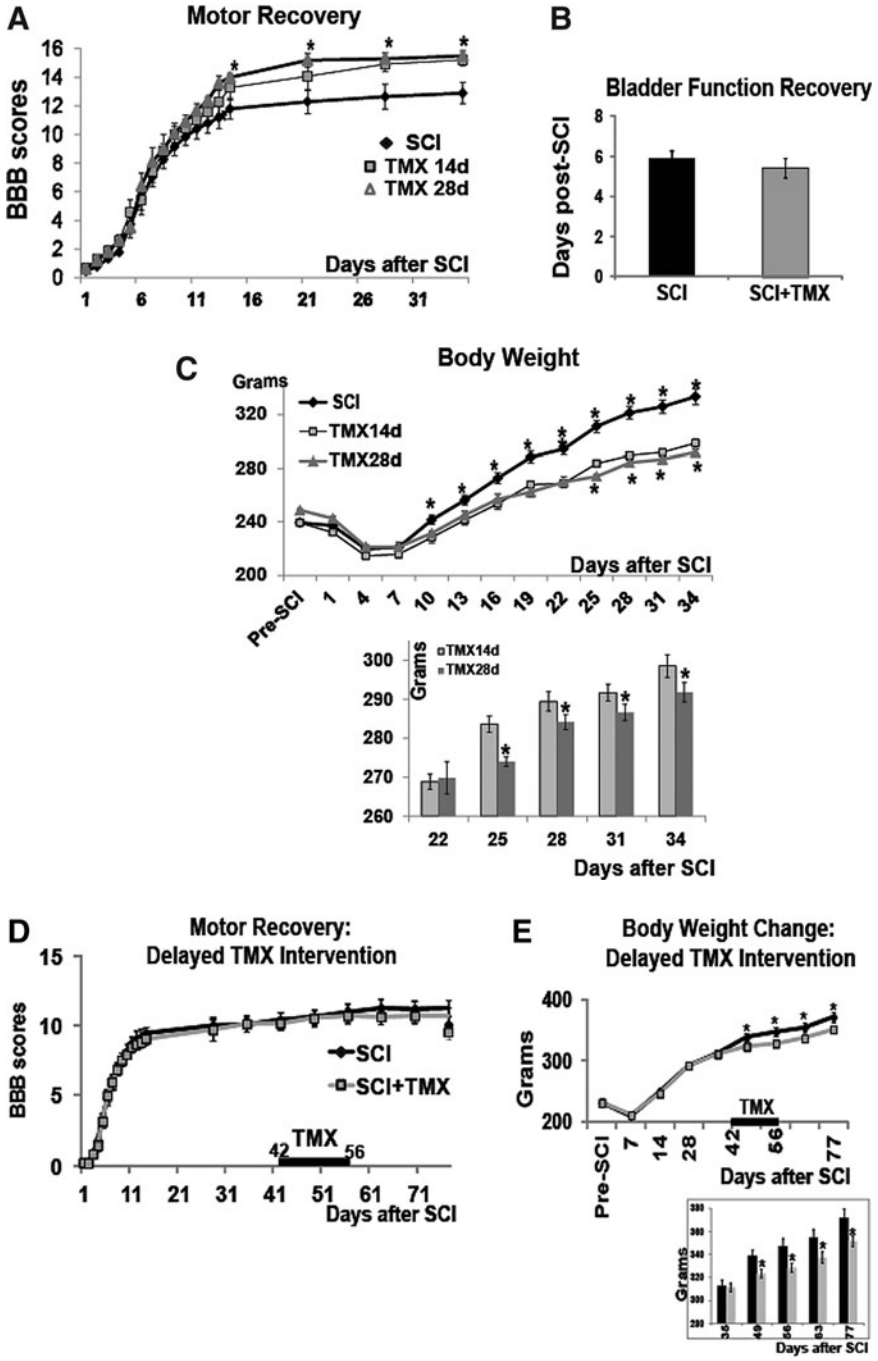

FIG. 1. Tamoxifen (TMX) improves locomotor recovery. **(A)** The effect of TMX (1mg/day/rat) on locomotor recovery of the hind limbs of moderately injured rats using Basso, Beattie, and Bresnahan (BBB) scoring (Y axis) over time (1 to 35 days after spinal cord injury [SCI]. 21 is the BBB score of uninjured rats). TMX was delivered for either 14 days (gray squares) or 28 days (gray circles). Black circles represent motor recovery of control SCI rats. Graph presents mean ± standard deviation (SD); $*=p<0.05$. **(B)** Bladder function recovery. Y-axis = days post-SCI. **(C)** Changes in body weight of SCI rats (grams) over time post-SCI. Bar graph represents the same data as in the graph above, but the Y-axis range is from 260 to 300 grams, so the changes between two TMX treatment paradigms (14 days and 28 days) are more apparent. Both graphs present mean ± SD; $*=p<0.05$. **(D)** Locomotor recovery of hind limbs of SCI rats treated with TMX (1mg/day/rat) starting at 52 days after SCI. Graph presents mean ± SD. **(E)** Body weight changes (grams) over time before (0–42 days post-SCI) and after TMX intervention (42–56 days). mean ± SD. $*=p<0.05$. Bar graph presents the same data, but with a re-scaled Y-axis.

with p values produced for each compared spot. Because of the large number of the spots (1119), we adjusted the p values for multiple-testing procedure, using the Benjamini-Hochberg model.[34] In brief, the method first sorts all p values in ascending order. Then every p value is modified to have a new (interim) value, $i*p_$value/N, where, i is the index (in the sorted data) of the original p value, and N is total number of the null hypothesis. The adjusted p values are determined as cumulative minima in the array of interim p-values. The BH adjustments to the p-values were done using the *p.adjust* function of R.[35]

Results

Acute TMX administration

TMX improved the locomotor recovery of SCI rats. SCI rats were divided into three experimental groups: (1) SCI rats that received no treatment ($n = 10$); (2) control SCI rats that received a placebo pellet releasing vehicle ($n = 10$); and (3) SCI rats that received TMX pellets ($n = 20$). We measured locomotor recovery of vehicle- and TMX-treated SCI rats using the BBB test (Fig. 1A). We did not find statistically significant differences in the BBB scores between SCI rats that received no treatment and those that received placebo pellets. Therefore, those two groups of SCI rats were combined into one control group ($n = 20$). In all graphs presented here, control group of SCI rats is labeled as ''SCI,'' while SCI rats treated with TMX are labeled as ''TMX.''

TMX was delivered daily (1 mg/rat) for either 14 days or 28 days; ($n = 10$/group). As shown in Figure 1A, both groups of TMX-treated SCI rats (14 and 28 day delivery), demonstrated a delayed, but significant improvement in hind-limb locomotion. Although improvements in BBB scores were similar, the 28-day TMX delivery group of SCI rats appeared to achieve faster locomotor recovery than the 14-day delivery group. The maximal improvement of ~ 3 BBB score units was achieved 35 days after SCI in both TMX-treated groups. In contrast to control SCI rats, all TMX-treated SCI rats showed a coordinated gait at 35 days after SCI. The same difference in the BBB scores at 28 and 35 days after SCI was confirmed by another experimenter, also blinded to drug treatments.

Bladder function recovery occurred at about six days post-SCI, in control SCI and all TMX-treated SCI rats (14-day and 28-day delivery groups were plotted together; Fig. 1B) Therefore, TMX did not affect bladder recovery of SCI rats.

It is well established that continuous administration of TMX induces a reduction in body weight.[36–39] Therefore, we measured the body weight of all SCI rats as an indicator of the effectiveness of TMX delivery via pellets. TMX-treated SCI rats had markedly and significantly reduced body weight versus control SCI rats (Fig. 1C). Further, weight gain in SCI rats treated with TMX for 14 days was accelerated beyond 22 days post-SCI (shown in the bar graph in Fig. 1C), compared with SCI rats treated with TMX for 28 days, indicating that this TMX effect remained for about one week after TMX pellets ceased to release the drug.

Delayed TMX administration

TMX did not affect the locomotor recovery of SCI rats. TMX pellets (1 mg/day/rat) were subcutaneously inserted 42 days after SCI, and delivered TMX for 14 days (until 56 days post-SCI). Similarly injured SCI rats were divided into three groups 42 days after SCI: 1) SCI rats that received no treatment ($n = 10$); 2) control SCI rats that received a placebo pellet ($n = 15$); and 3) SCI rats that received TMX pellets ($n = 19$).

In contrast to acute TMX administration, delayed TMX delivery did not improve locomotor recovery (Fig. 1D; SCI rats that received placebo pellet and SCI rats that received no treatment were again combined into one group). Similar to acute TMX intervention, delayed delivery of TMX also suppressed the weight gain in SCI rats (Fig. 1E), indicating that the lack of beneficial TMX effects on locomotor recovery of SCI rats did not result from ineffective TMX pellets.

Proteomic analyses

TMX affected the abundance of proteins expressed in oligodendrocytes and astrocytes. Proteomic analysis was performed with proteins (total cell extracts) isolated from the lesion site (T10) 35 days after SCI in three experimental groups: 1) SCI rats treated with TMX for four weeks ($n = 5$), 2) control SCI rats (no treatment; $n = 5$); and 3) naïve age-matched rats that received no treatment ($n = 5$). The protein spots from all gels were matched, and an abundance value for group 1 calculated versus naïve and control SCI rats. Fluorescence staining revealed 1118 spots; only spots whose abundance satisfied the following criteria were selected for identification by mass spectrometric analysis (MS): 1) abundance changed significantly after both SCI (uninjured vs. SCI; $p < 0.05$), and TMX treatment (SCI vs. TMX; $p < 0.05$), or 2) abundance did not change significantly after SCI (uninjured vs. SCI; $p \geq 0.05$) but it did after TMX treatment (SCI vs. TMX; $p < 0.05$).

Our statistical analysis identified 25 spots that were excised and processed for MS identification; no proteins were found where abundance was affected by TMX but not affected by SCI, suggesting that TMX predominantly affected the abundance of proteins altered by SCI. The identities of the 25 selected spots are shown in Table 2. The abundance of the first ten proteins in Table 2 was significantly decreased in SCI rats (fold change SCI vs. naïve < 1), and significantly increased in TMX-treated SCI rats (fold

Table 1. Antibodies Used in Western Blots

	Primary Ab			*Secondary Ab*		
Name	*Animal*	*Company/cat #*	*Dilution*	*Animal*	*Company/cat #*	*Dilution*
2′,3′-cyclic-nucleotide 3′-phosphodiesterase	Mouse	Abcam/Ab6319	1:500	Goat	Southern Biotech# 1034-05	1:5,000
Myelin basic protein - oligodendrocyte marker	Rabbit	Abcam/Ab 2404	1:500	Goat	Southern Biotech# 4052-05	1:5,000
Myelin oligodendrocyte glycoprotein	Goat	Abcam/Ab 28766	1:1,000	Donkey	R&D System# HAF 109	1:3,000
Phosphorylated neurofiilament	Mouse	Covance/SMI-31R	1:1,000	Goat	Southern Biotech# 1034-05	1:5,000
Nonphosphorylated neurofiilament	Mouse	Covance/SMI-32R	1:1,000	Goat	Southern Biotech# 1034-05	1:5,000
Glial fibrillary acidic protein	Mouse	Millipore/MAB360	1:8,000	Goat	Southern Biotech# 1034-05	1:5,000
Aquaporin 4	Rabbit	Millipore/AB 3594	1:5,000	Goat	Southern Biotech# 4052-05	1:5,000
Vimentin	Rabbit	Epitomic/2707-1	1:3,000	Goat	Southern Biotech# 4052-05	1:5,000
Iba-1	Rabbit	Wako/016-20001 (WB)	1:500	Goat	Southern Biotech# 4052-05	1:5,000
β-actin	Mouse	Sigma/A5441	1:80,000	Goat	Southern Biotech# 1034-05	1:5,000

Ab, antibody.

Table 2. Proteomics Analysis

	Fold change SCI vs. N	*Fold change TMX vs. SCI*	*Acession number*	*MW (KDa)*	pi	*Expectation Swiss*	*Score NCBI*	*Spot No.*
SCI-induced decreases								
Enoyl-CoA hydratase domain-containing protein 1 OS=Rattus norvegicus GN=Echdc1 PE=1 SV=1	0.35	2.4	Q6AYG5	31	6.5	0.099763116	0.997631157	736
Pyruvate kinase isozymes M1/M2 OS=Rattus norvegicus GN=Pkm2 PE=1 SV=3	0.5	1.3	P11980	58	5.7	1.99054E-17	1.99054E-16	103
2',3'-cyclic-nucleotide 3'-phosphodiesterase OS=Rattus norvegicus GN=Cnp PE=1 SV=2	0.5	1.2	P13233	45	5.9	2.50594E-14	2.50594E-13	498
Peroxiredoxin-6 OS=Rattus norvegicus GN=Prdx6 PE=1 SV=3	0.55	1.7	O35244	19	6.1	25.05936168	15.8113883	953
COP9 signalosome complex subunit 8 OS=Rattus norvegicus GN=Cops8 PE=2 SV=1	0.55	1.4	Q6P4Z9	21	5.2	0.000397164	0.000315479	908
Alpha-soluble NSF attachment protein OS=Rattus norvegicus GN=Napa PE=1 SV=2	0.7	0.8	P54921	34	5.3	0.199053585	1.990535853	682
Stathmin OS=Rattus norvegicus GN=Stmn1 PE=1 SV=2	0.7	1.2	P13668	18	5.6	1.99054E-05	7.92447E-05	987
Histidine triad nucleotide-binding protein 1 OS=Rattus norvegicus GN=Hint1 PE=1 SV=5	0.8	1.2	P62959	15	6.3	1.990535853	7.924465962	1063
L-lactate dehydrogenase B chain OS=Rattus norvegicus GN=Ldhb PE=1 SV=2	0.8	1.2	P42123	31	5.7	3.97164E-05	0.000397164	728
Nucleolar RNA helicase 2 OS=Rattus norvegicus GN=Ddx21 PE=2 SV=1	0.8	1.2	Q3B8Q1	31	6.2	1.255943216	3.971641174	734
SCI-Induced Increases								
Ubiquitin-40S ribosomal protein S27a OS=Rattus norvegicus GN	7.6	0.2	P62982	>250	6.7	0.0000005	9.97631E-08	1145
Fibroblast growth factor 23 OS=Rattus norvegicus GN=Fgf23 PE=2 SV=1	2.8	0.6	Q8VI82	21	9.6	0.629462706	6.294627059	905
Glial fibrillary acidic protein OS=Rattus norvegicus GN=Gfap PE=1 SV=2	2.2	0.7	P47819	48	5.4	1.25594E-60	1.25594E-59	1321
Pleckstrin homology domain-containing family B member	2	0.6	Q9WU68	13	7.7	15.8113883	9.976311575	1097
Glial fibrillary acidic protein OS=Rattus norvegicus GN=Gfap PE=1 SV=2	1.9	1.4	P47819	60	5.4	7.92447E-35	7.92447E-34	1210
Fibroblast growth factor 23 OS=Rattus norvegicus GN=Fgf23 PE=2 SV=1	1.8	0.6	Q8VI82	10	5.3	7.924465962	15.8113883	1138
Glial fibrillary acidic protein OS=Rattus norvegicus GN=Gfap PE=1 SV=2	1.8	0.8	P47819	49	5.3	1.25594E-89	1.99054E-89	1317
Protein disulfide-isomerase A3 OS=Rattus norvegicus GN=Pdia3 PE=1 SV=2	1.6	0.8	P11598	65	5.7	2.50594E-22	2.50594E-21	364
CCR4-NOT transcription complex subunit 10 OS=Rattus norvegicus GN=Cnot10 PE=2 SV=1	1.5	0.8	Q5XIA4	39	6.1	2.505936168	9.976311575	577
Splicing factor U2AF 26 kDa subunit OS=Rattus norvegicus GN=U2af1l4 PE=2 SV=1	1.4	1.3	Q7TP17	40	5.8	39.71641174	3.971641174	571
Fructose-bisphosphate aldolase C OS=Rattus norvegicus GN=Aldoc PE=1 SV=3	1.3	0.9	P09117	37	7	5E-40	5E-39	602
Glutathione S-transferase Mu 5 OS=Rattus norvegicus GN=Gstm5 PE=1 SV=3	1.3	0.85	Q9Z1B2	27	6.1	0.000629463	0.006294627	818
Mitogen-activated protein kinase 3 OS=Rattus norvegicus GN=Mapk3 PE=1 SV=5	1.3	0.7	P21708	45	6.2	9.97631E-14	7.92447E-13	488
D-3-phosphoglycerate dehydrogenase OS=Rattus norvegicus GN=Phgdh PE=1 SV=3	1.2	0.9	O08651	57	6	0.000792447	0.007924466	393
Fascin OS=Rattus norvegicus GN=Fscn1 PE=1 SV=2	1.2	0.8	P85845	58	6.2	0.5	5	384

MW, molecular weight; No., number; SCI, spinal cord injury; N, naive; TMX, tamoxifen; NCBI, National Center for Biotechnology Information.

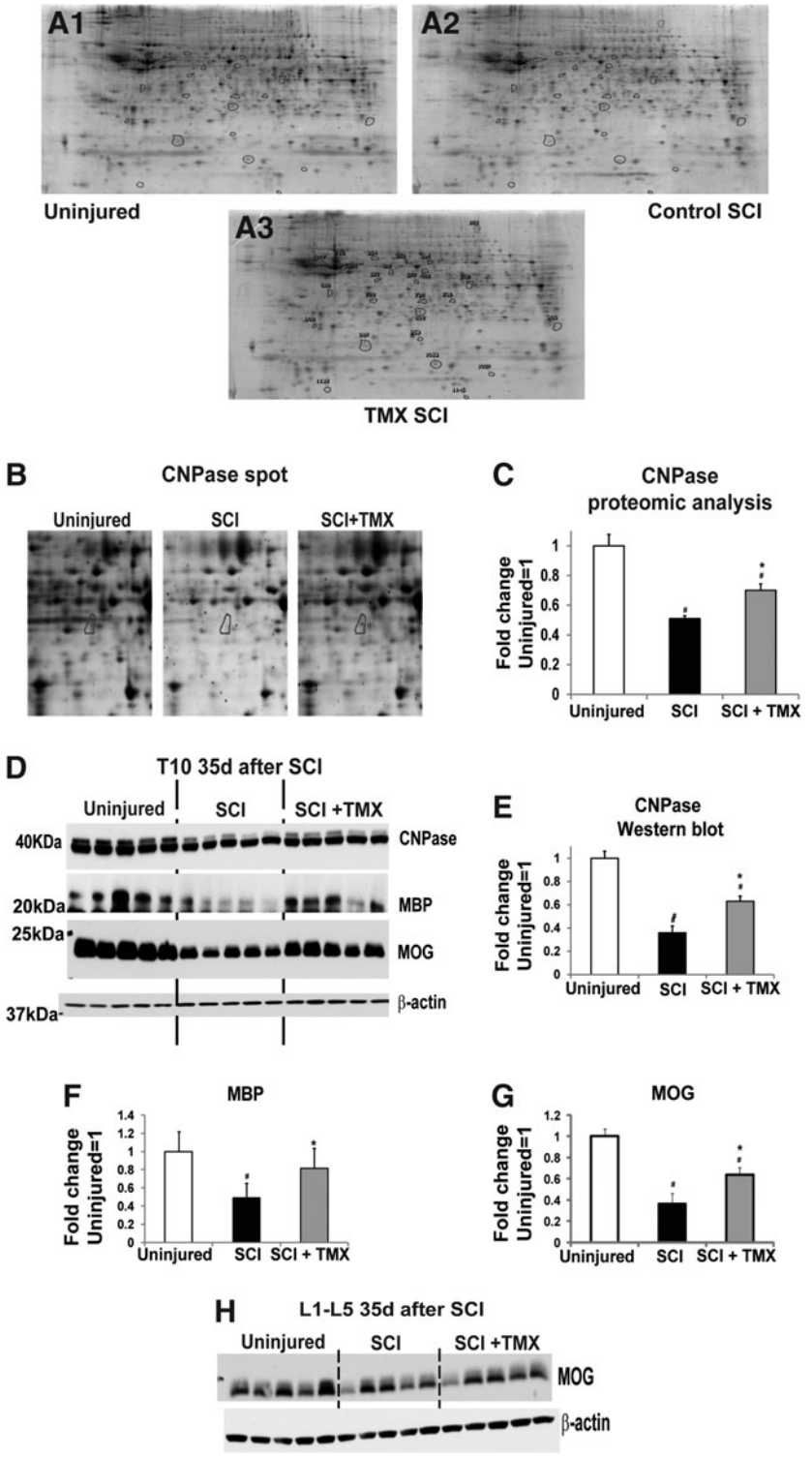

FIG. 2. Tamoxifen (TMX) restores myelin loss at the lesion site. **(A)** Representative images of 2D gels from three experimental groups: uninjured, **(A1);** control spinal cord injury (SCI; **A2)** and TMX-treated SCI rats **(A3);** we used total cell extracts from the 10th thoracic segment (T10), 35 days after SCI. Spots in A3 are labeled with numbers corresponding to the ''Spot No.'' in Table 2. **(B)** Enlarged area of three representative 2D gels containing spot No. 498 (i.e., 2′,3′-cyclic-nucleotide 3′-phosphodiesterase [CNP-ase]; marked with blue circles). **(C)** Bar graph showing quantitative analysis of abundance values for spot No. 498 (CNP-ase) in proteomic analysis in three experimental groups ($n = 5$ rats/group). All values were normalized to the mean value obtained in uninjured samples ($= 1$). Mean ± standard deviation (SD); $^{\#}$denotes a significant difference between uninjured and SCI groups; *a significant difference between SCI and SCI + TMX groups; $^{\#,*} = p < 0.05$. **(D)** Western blot analysis of different myelin proteins (CNP-ase, myelin basic protein [MBP], and myelin oligodendrocyte glycoprotein [MOG]) at T10, 35 days after SCI in three experimental groups ($n = 5$/group). β-actin was analyzed in all Western blots as a loading control, in addition to the Ponceau staining. **(E)** Quantitative analysis of CNP-ase Western blots. Mean ± SD; $^{\#,*}p < 0.05$. **(F)** Quantitative analysis of MBP Western blots. Mean ± (SD); $^{*} = p < 0.05$. **(G)** Quantitative analysis of MOG Western blots. Mean ± SD; $^{\#,*}p < 0.05$. **(H)** MOG levels were also measured in lumbar segments 35 days after SCI using Western blots ($n = 5$/group). No changes in MOG levels were detected among the three experimental groups.

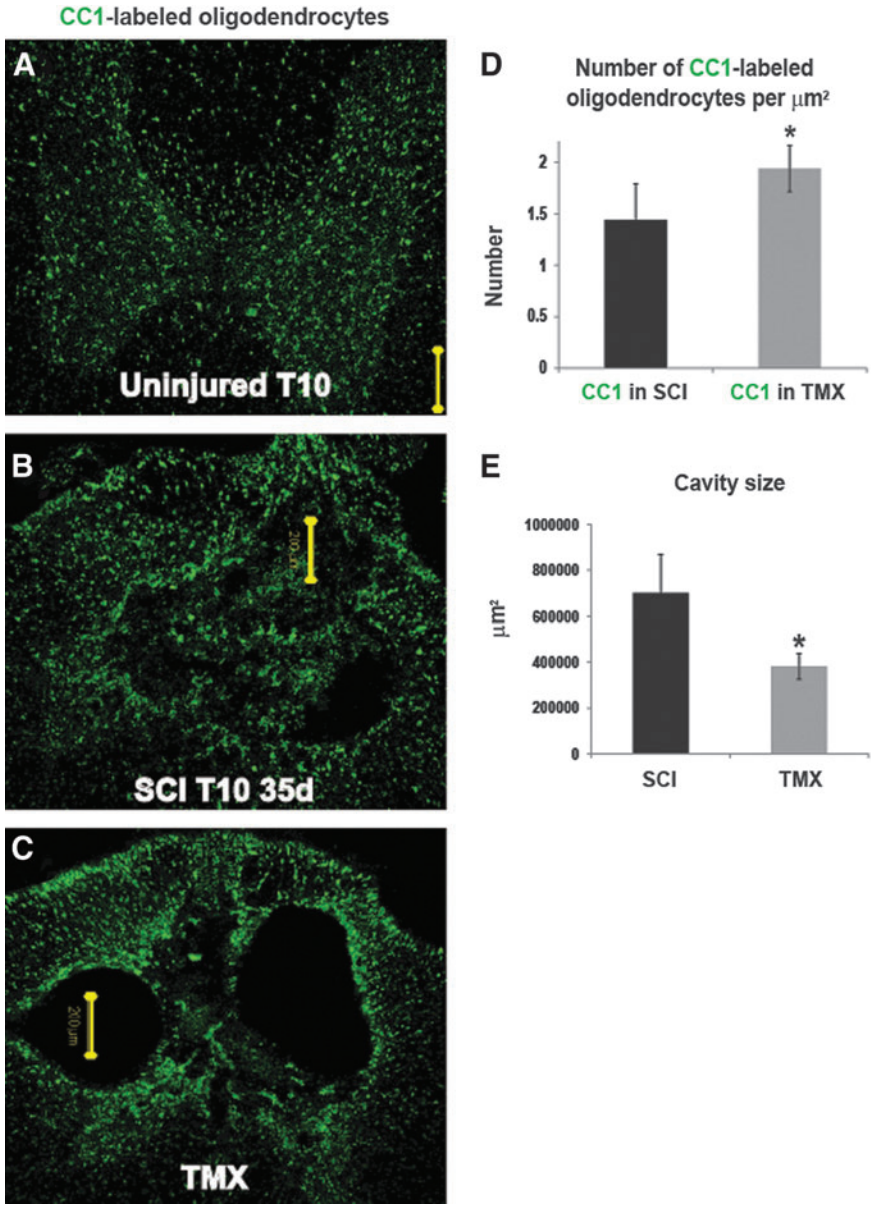

FIG. 3. Tamoxifen (TMX) spares oligodendrocytes and reduces cavitation. Representative confocal images of the CC1-immunolabeling at the 10th thoracic segment (T10), 35 days after spinal cord injury (SCI), in three experimental groups, an age-matched uninjured rat, **(A),** control SCI, **(B)** and TMX-treated SCI group **(C)**. Calibration line: 200 μm. Calibration line was positioned within the cavity to indicate its size. **(D)** Quantitative analysis of the number of CC1-labeled cells per μm^2 in control and TMX-treated groups. Five random sections of T10 sections from each group were chosen for the analysis; $n = 5$ rats/experimental group. Mean ± standard deviation; $*p < 0.05$. **(E)** Cavity sizes were determined as described in the Methods section (also see supplementary material). Color image is available online at www.liebertpub.com/neu

change TMX vs. SCI > 1). We also identified 15 proteins (see Table 2) where levels were significantly increased in SCI rats (fold change SCI vs. naïve > 1), and then significantly changed in TMX-treated SCI rats.

Among proteins where abundance was significantly decreased after SCI and then partially restored by TMX, we found markers of oligodendrocytes, such as 2′,3′ -cyclic nucleotide 3′-phosphodiesterase (CNPase),[40] and of oligodendrocyte progenitors (stathmin),[41] as well as myelin (enoyl co-A).[42] These findings indicate a beneficial effect of TMX on oligodendrocytes and myelin levels, of which loss at the lesion site substantially contributes to functional impairment after SCI.

Among proteins that were significantly elevated after SCI and then decreased by TMX treatment, we found markers of astrocytes and their activation, such as glial fibrillary acidic protein (GFAP isoforms), fascin (intermediate filaments bound to GFAP[43] or D-3-phosphoglycerate dehydrogenase,[44] which suggests that TMX ameliorates the activation of astrocytes at the lesion site. To confirm the results of our proteomic analysis we performed Western blots (Fig. 2 and Fig. 4).

TMX increased myelin levels at the lesion site

In Figure 2A, we show representative images of 2D gels: A1, age-matched uninjured T10; A2, T10 in control SCI (35 days after

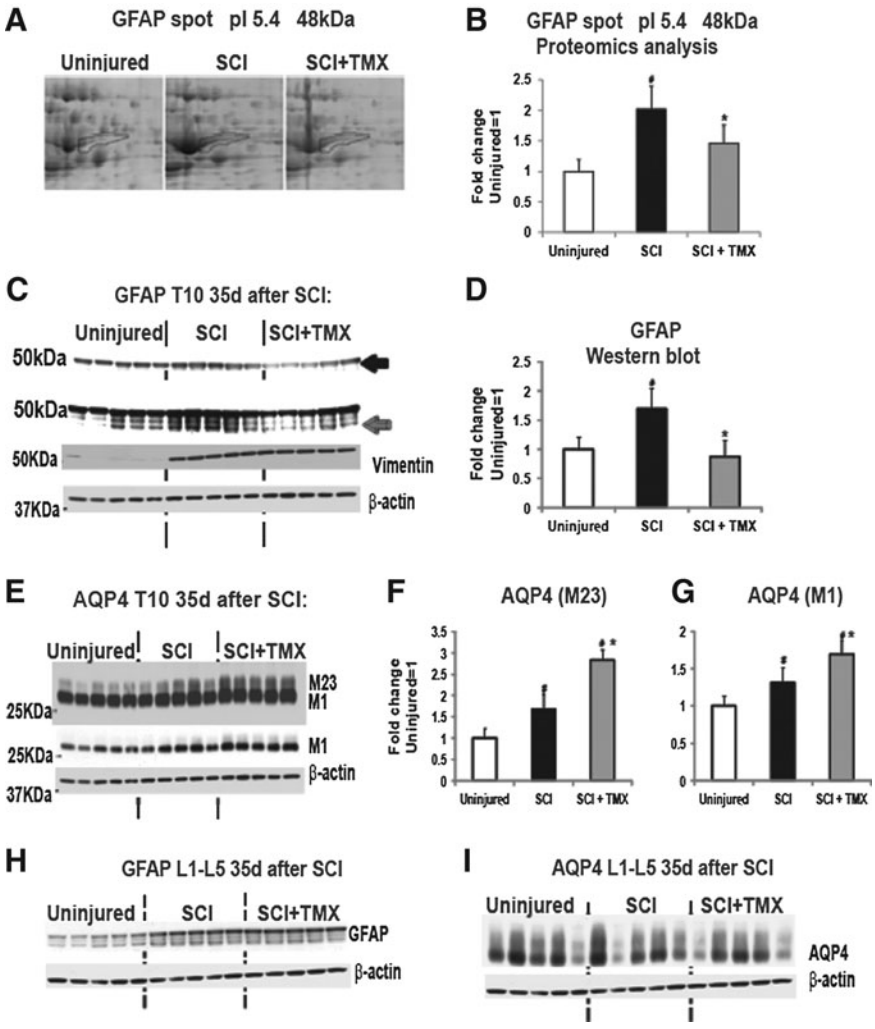

FIG. 4. Tamoxifen (TMX) affects reactive astrocytes. **(A)** Enlarged area of representative 2D gels containing spot No. 1321 (48kDa GFAP, marked in blue) from three experimental groups: uninjured, control spinal cord injury (SCI), and TMX-treated SCI. **(B)** Bar graph represents quantitative analysis of abundance values for Spot No. 1321 (48kDa GFAP, pI 5.4: $n=5$ rats/group). All values were normalized to the mean value for uninjured samples ($=1$). Mean ± standard deviation (SD); $^{\#,*}=p<0.05$. **(C)** Western blot analysis of glial fibrillary acidic protein (GFAP) and vimentin levels at the tenth thoracic segment (T10), 35 days after SCI. GFAP bands marked with a black arrow represent lower exposure time to demonstrate changes in ~50 kDa GFAP band, while multiple bands visible with longer exposures (marked with gray arrow) represent changes in GFAP bands/isoforms whose MW were below 50kDa. **(D)** Quantitative analysis of all GFAP bands obtained in Western blots. Mean ± SD; $^{\#,*}=p<0.05$. **(E)** Western blot analysis of aquaporin 4 (AQP4) at T10, 35 days after SCI in three experimental groups; $n=5$ /group. The upper image represents a longer exposure that shows changes in the higher MW band (M23 isoform), while the lower Western blot image shows the same Western blot, but with a lower exposure time, so changes in the M1 isoform are clearly visible. **(F)** Quantitative analysis of the M23 AQP4 isoform measured using Western blots. Mean ± SD; $^{\#,*}=p<0.05$. **(G)** Quantitative analysis of the M1 AQP4 isoform. Mean ± SD; $^{\#,*}p<0.05$. **(H)** GFAP levels were also measured (using Western blots) in lumbar segments 35d after SCI (n = 5/group). **(I)** Western blot analysis of AQP4 levels in lumbar segments 35 days after SCI.

SCI); and A3, T10 in SCI rats treated with TMX (35 days after SCI). Figure 2B presents an enlarged region containing spot #498 (identified as CNPase, a myelin-associated enzyme). The bar graph in Figure 2C shows quantitative analysis of normalized CNPase abundance levels obtained from proteomic analysis in 15 2D gels ($n=5$/group), indicating a significant decrease in CNPase levels at the lesion site 35 days after SCI (#; $p<0.05$) and a partial but significant reversal in TMX-treated SCI rats (*; $p<0.05$). We also used Western blots to measure CNPase protein levels at T10 in naïve, control SCI, and TMX-treated SCI rats ($n=5$/group; Fig. 2D and Fig. 2E). TMX treatment was identical in all SCI rats used for both proteomic and Western blot analyses. All Western blot analyses were repeated twice by two experimenters, and only results confirmed in two independent experiments are presented here. Consistent with our proteomic analyses, Western blots also showed SCI-induced CNPase decreases (an ~40 kDa band, Fig. 2D) at T10 35 days after SCI (#; $p<0.05$) and a partial but significant reversal with TMX treatment (*; $p<0.05$; Fig. 2D and Fig. 2E). We found that CNPase levels were decreased at the lesion site by ~50% in proteomic analyses (Fig. 2C), and by ~60% in Western blot analyses (Fig. 2D and Fig. 2E). TMX treatment significantly increased CNPase levels at the lesion site by 30% in Western blots, and by 20% in the proteomics study.

To further confirm the beneficial effect of TMX on myelin loss after SCI, we also measured protein levels of myelin basic protein (MBP), the most abundant myelin protein in mature

oligodendrocytes/axons. Using Western blots, we found a ~50% decrease in MBP levels at the lesion site 35 days after SCI (#; $p < 0.05$; Fig. 2F), consistent with our CNPase analyses (Fig. 2C and Fig. 2E). We also found that TMX significantly increased MBP levels by 20% (*; $p < 0.05$, Fig. 2D). The late-appearing myelin oligodendrocyte glycoprotein (MOG) is a marker of the final steps in the myelination processes. MOG levels were significantly decreased by >60% at the lesion site 35 days after SCI (#; $p < 0.05$; Fig. 2 D and Fig. 2G), and significantly restored in TMX-treated SCI rats, by ~20% (*; $p < 0.05$; Fig. 2D and Fig. F), in agreement with the results in Figures 2C, 2E, and 2F.

We also tested if TMX treatment affected myelin levels in lumbar segments (pooled L1-L5). Lumbar segments directly control hind-limb locomotion.[45,46] Therefore, in addition to myelin changes at the lesion site, myelin changes in lumbar segments also could affect the recovery of hind-limb function after SCI. As shown in Figure 2H, we analyzed MOG levels in lumbar segments of the same SCI rats whose T10 segments were used for the analyses

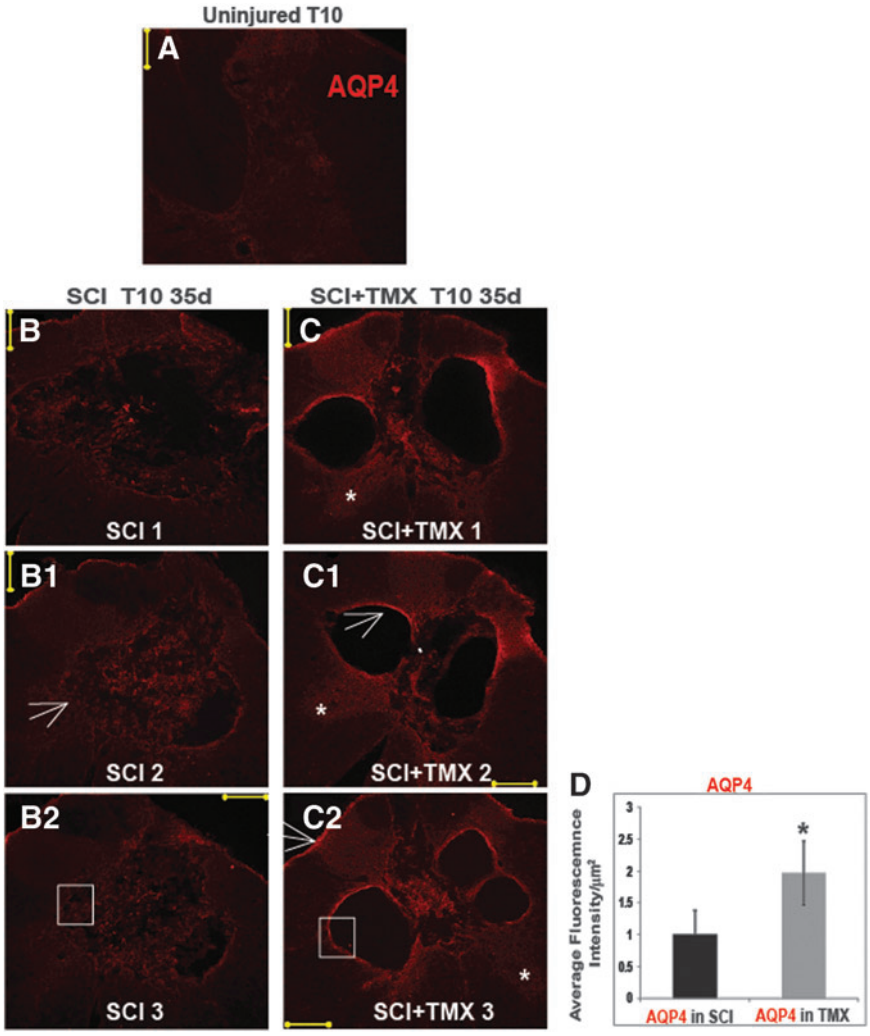

FIG. 5. Aquaporin 4 (AQP4) and the organization of the lesion wall. **(A)** AQP4 immunolabeling in the uninjured 10th thoracic segment (T10) segment of an age-matched uninjured rat. Calibration line: 200 μm. **(B-B2)** Representative confocal image of AQP4 immunolabeling in a control spinal cord injury (SCI) rat (T10, 35 days after SCI), three sections were taken 40 μm apart**. (C-C2)** Representative 3 sections from the lesion site of a tamoxifen (TMX)-treated SCI rat. White stars mark better preservation of gray matter in TMX-treated SCI rats, even when the size of the cavities did not significantly differ from a control SCI rat. White arrows: the lesion wall in a TMX-treated SCI rat demonstrated high AQP4 levels, in contrast to the lesion border of a control SCI rat. The organization of the lesion wall and the intensity of AQP4 immunolableing within the lesion border were similar to the organization and AQP4 immunolableing in glia limitans in a TMX-treated SCI rat (thin white arrow in **C2**). **(D)** Fluorescence Intensity quantitative analysis of AQP4 labeling shows two-fold increases in TMX-treated SCI rats. Five random sections were chosen from each lesion site ($n = 5$/group). The intensity was normalized to SCI = 1. Mean ± SD; * = $p < 0.05$. **(E)** High magnification image of AQP4 labeling in a segment of the lesion wall in a control SCI rat (area of the lesion wall is marked with white square in B2). Calibration line: 50 μm. The image of AQP4 labeling on the right represents a 3D rendering (done by z-stacks acquisition of confocal images) of a lesion wall segment facing the cavity (cavity is marked with the yellow star) and demonstrates disorganized AQP4-expressing astrocytes; nuclei were labeled in blue with 4′,6-diamidino-2-phenylindole, dihydrochloride. **(F)** The astrocytic organization of the lesion walls in a TMX-treated SCI rat resembled the astrocytic organization in glia limitans of an uninjured rat **(G)**; yellow star marks the side facing the subarachnoid CSF). Calibration line: 20 μm. Color image is available online at www.liebertpub.com/neu

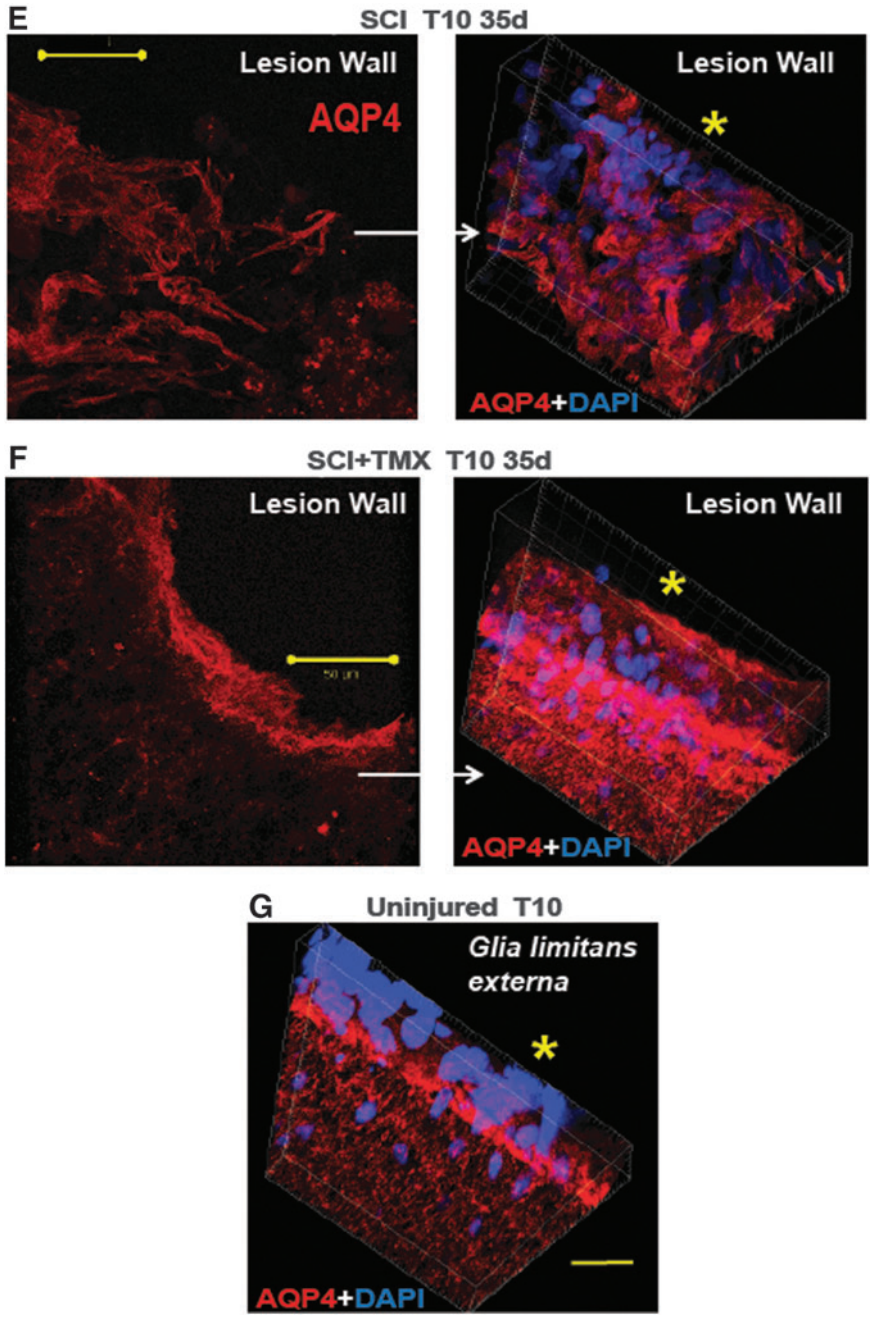

FIG. 5. (Continued)

shown in Figure 2D. MOG levels in the lumbar segments of SCI rats were not significantly affected by either SCI or TMX, suggesting that TMX does not affect myelin levels in the absence of injury-induced processes, in agreement with our proteomic analysis showing no effect of TMX on proteins unaltered by SCI.

TMX spared oligodendrocytes

The CC1 antibody recognizes adenomatus polyposis coli, and is a marker of oligodendrocyte cell bodies without labeling myelin.[47] CC1-labeled oligodendrocytes were assessed in three groups of rats: 1) naïve rats (Fig. 3A); 2) SCI rats that received vehicle Fig. 3B); and 3) SCI rats that received TMX (1 mg/day) for 14 days (Fig. 3C; $n=5$/group). We found significantly increased CC1 immunolabeling in all TMX-treated SCI rats (Fig. 3D), indicating an $\sim$20% increase in the number of mature oligodendrocytes/μm^2 in TMX-treated SCI rats, consistent with $\sim$20% preservation of myelin (Fig. 2). Here, we show increased CC-1 labeling in TMX-treated SCI rats even when cavities at the lesion site had sizes similar to those in control SCI rats (Fig. 3B and Fig. 3C), suggesting that TMX had a sparing effect on oligodedendrocytes independent of reduced cavitation. Our quantitative assessment of cavity sizes in AQP4-immunolabeled lesion sites (AQP4 delineated cavity borders; see Fig. 5) showed significant ($*p=0.0035$) 1.83-fold smaller lesion sizes in TMX-treated injured spinal cords ($n=5$/group; Fig. 3F).

TMX altered astrocytic activation at the lesion site

Proteomic analysis identified 48 and 49 KDa GFAP bands (Table 2, Fig. 4A and Fig. 4B) as being significantly increased after SCI by ~80-120% (#; $p < 0.05$; Table 2; Fig. 4B), and decreased by ~50% in TMX-treated SCI rats (*; $p < 0.05$; Table 2; Fig. 4B). As shown in Figure 4B, $GFAP_{48kDa}$ levels in TMX–treated SCI rats were indistinguishable from those in uninjured spinal cords, suggesting that TMX treatment abolished astrocytic activation at the lesion site. Western blot analysis (Fig. 4C) confirmed the proteomic findings. SCI-induced increases in several GFAP bands, including the ~50kD band (marked with black arrow) and GFAP bands with lower molecular weight (MW; between 45 and 50 kDa, marked with gray arrow) were seen in the same Western blots with a longer exposure time. We quantified all GFAP bands together (Fig. 4D). SCI induced significant increases in GFAP bands, by ~70% (#; $p < 0.05$). TMX treatment abolished the SCI-induced increases in GFAP levels (*; $p < 0.05$; Fig. 4D), although it more prominently affected the intensity of the lower MW bands (< 50kDa; Fig. 4C). Interestingly, vimentin, another intermediate filament protein strongly increased in activated astrocytes after SCI (Fig. 4C), was not affected by TMX, suggesting that TMX selectively affects different targets in reactive astrocytes in injured spinal cords.

AQP4 is another exclusively astrocytic protein that is significantly upregulated in activated astrocytes in chronically injured spinal cords,[48] consistent with our findings here (Fig. 4E, 4F, and 4G). We also found that AQP4 levels were even more increased in TMX-treated SCI rats (Fig. 4E, 4F, and 4G). As shown in Figure 4F, we found that TMX treatment elevated levels of the AQP4 M23 isoform by ~50%, and of the M1 isoform by ~20% (Fig. 4G) at the lesion site 35 days after SCI.

In contrast to unchanged myelin levels in lumbar cord segments, GFAP levels in L1-L5 were mildly but significantly increased 35 days after SCI (Fig. 4H). However, TMX did not alter the GFAP levels, indicating that pathways upstream of the GFAP increases in lumbar segments are likely different from the signals that trigger GFAP increases at the lesion site. AQP4 levels in lumbar segments were unaffected by SCI (Fig. 4I), again suggesting that GFAP and AQP4 do not share the same upstream processes. AQP4 levels in lumbar segments were not altered by TMX (Fig. 4I), consistent with TMX affecting only injury-induced processes.

TMX altered the organization of cavity walls delineated by AQP4-expressing astrocytes

The most surprising result of the AQP4 immunolabeling at the lesion sites in control versus TMX-treated SCI rats was the difference in the shape of the cavities delineated by AQP4-labeled astrocytes. Figures 5B-B2 and 5C-C2 represent three sections 40 microns apart taken from the same T10 segments of control (B-B2) and TMX-treated SCI rats (C-C2). Cavities in TMX-treated SCI rats were more rounded, with walls consisting of densely packed AQP4-expressing astrocytes (white arrow in Fig. 5C1), whereas the cavities in control SCI rats were irregularly shaped with unorganized, partially opened walls (white arrow in Fig. 5B1). The same result was obtained in all analyzed control- and TMX-treated SCI rats ($n = 5$/group). High magnification images and the corresponding 3D renderings of lesion wall segments (labeled with white squares in Fig. 5B2 and 5C2) in control- and TMX-treated SCI rats (Fig. 5E and Fig. 5F) show well-organized cavity walls in TMX-treated SCI rats, with densely packed astrocytes abundantly expressing AQP4 that closely resembled the organization of the glia limitans externa (Fig. 5G).

TMX prevented spreading of cells into cavities

Well-organized lesion walls in TMX-treated SCI rats were associated with cavities devoid of cells (with DAPI- stained nuclei; Fig. 5C-C2 and Fig. 6B, 6D, and 6F), in contrast to cavities in control SCI rats (Fig. 5B-B2 and 6A, 6C, and 6E). We quantified DAPI-labeled nuclei only within the lesion in control- ($n = 5$) and TMX-treated SCI rats ($n = 5$; see Fig. 6E and 6F), and found that control SCI rats had ~3 fold more nuclei/μm^2 than TMX-treated SCI rats (Fig. 6G). Figures 6E and 6F are representative examples of cell infiltration within cavities in control and TMX-treated SCI rats, respectively. More interestingly, we found that cavity walls characterized by high AQP4 levels and glia limitans-like organization (thin white arrows in Fig. 6B) were associated with little or no cell penetration into the lesion cavity, not only in TMX-treated SCI rats (thin white arrow in Fig. 6F), but also in control SCI rats (thin white arrows in Fig. 6A and 6E), although such an organization of cavity walls was rare in control SCI. Conversely, segments of disorganized lesion walls in TMX-treated SCI rats that were not characterized by high AQP4 levels (thick white arrows in Fig. 6B and 6F) also were associated with infiltration of cells into the lesion. Although we have not performed a detailed characterization of cells infiltrating into the cavities, we identified CC-1 labeled cells (see Fig. 3B), AQP4-labeled cells (Fig. 6A) but also immature radial glia–like reactive astrocytes labeled with 3CB2 antibody and reactive microglia labeled with Iba-1 (Fig. 6H).

Discussion

Translational potential of tamoxifen

Based on the criteria outlined in the review by Tator and colleagues[49] and Guest and colleagues,[50] we summarized our results in Table 3, which suggest that TMX may be a promising intervention for the treatment of SCI. For example, TMX readily crosses the blood-brain barrier,[51–53] and therefore can be systemically administered, which has a clear clinical advantage. Further, the safety profile of TMX has been well established in the past four decades. TMX is approved by the United States Food and Drug Administration not only for the long-term (five-year) daily treatment of breast cancer patients but is also safe enough to be approved as a long-term preventive agent in women at high-risk for breast cancer. Adverse effects of TMX (increased risk of endometrial cancer and thromboembolic diseases; ~1.2 cases per 1000 women) strongly depend on the duration of its use.[54] Therefore, the short-term TMX therapy proposed here may be considerably safe, particularly in male SCI patients, who constitute ~80% of all SCI patients. Our analyses also supported the safety of 1mg/kg TMX administered for two weeks to SCI rats; it did not cause adverse liver changes and it did not affect proteins in uninjured spinal cords.

Even though the same TMX intervention paradigm used in our experiments was not repeated by another research group (reproducibility increases translational potential of pharmacological interventions)[49] beneficial effect of a similar TMX dose (5mg/kg) on motor recovery of SCI rats has already been shown by Tian and colleagues,[23] who administered one TMX injection 30 min post-SCI. Although our study tested the effect of TMX in a more clinically applicable time window (starting 2 h after SCI), the results of both studies suggest that TMX has a clear translational potential as a pharmacological intervention for SCI. Further, pharmacological interventions currently in clinical trial for SCI (minocycline or riluzol) or interventions that have translational potential (nimodipine, magnesium sulfate, or glyburide)[49] have demonstrated either smaller or equivalent improvements in locomotor recovery as

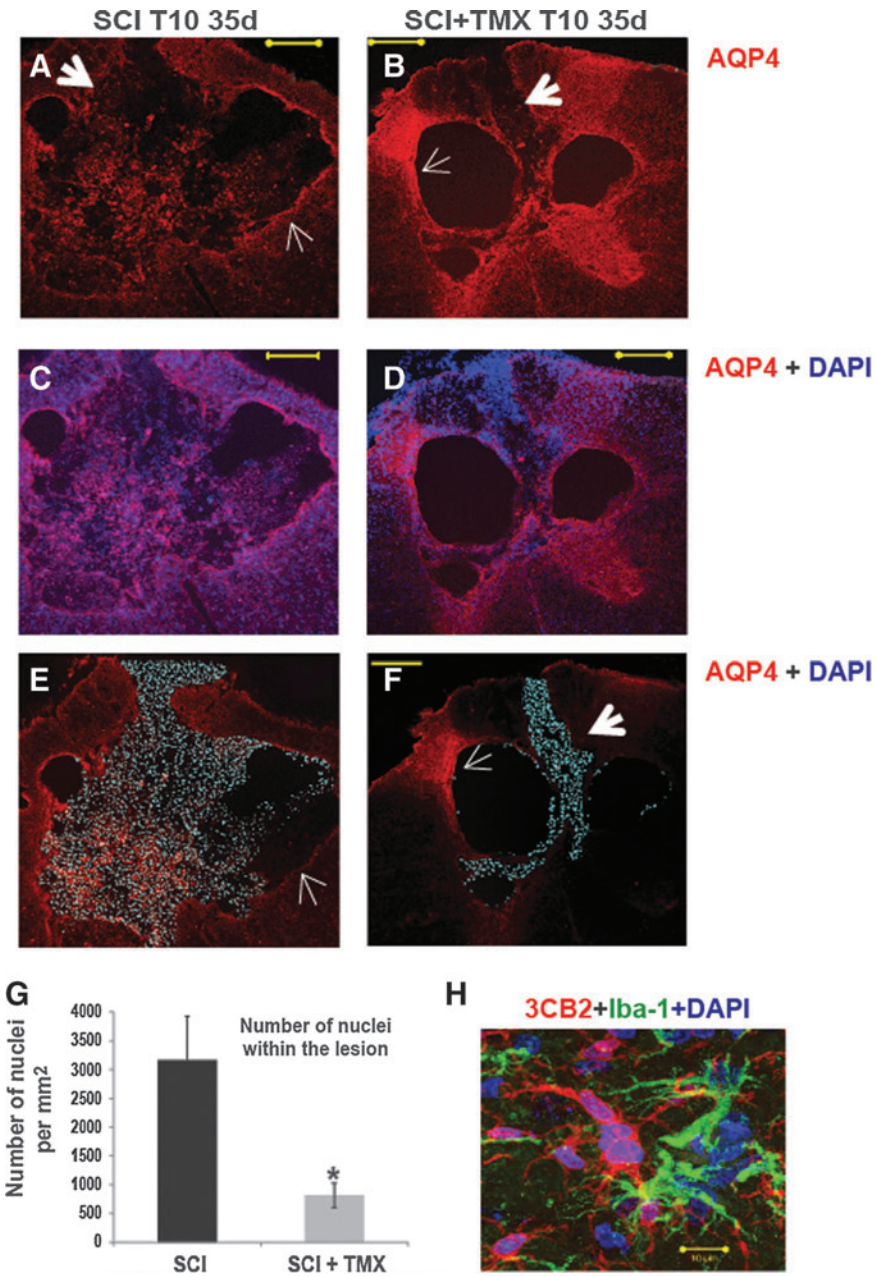

FIG. 6. Spreading of cells within the lesion. **(A)** A representative image of aquaporin 4 (AQP4) immunolabeling at the lesion site in an spinal cord injury (SCI) rat. Thick white arrow: segments of disorganized lesion border with low intensity AQP4 labeling. Thin white arrow: more organized lesion border were associated with higher AQP4 levels. Calibration line: 200 μm. **(B)** AQP4 labeling at the lesion site in a tamoxifen (TMX)-treated SCI rat. **(C)** AQP4 (red, image A) co-labeled with nuclei (blue, 4′,6-diamidino-2-phenylindole, dihydrochloride [DAPI]). **(D)** Co-labeling of AQP4 (red) and nuclei (blue, DAPI). **(E)** DAPI channel (pseudo-colored in cyan) showing only the nuclei (cells) within the lesion in a SCI rat (the same section as presented in A and C). We found widespread cell infiltration within the lesion of all control SCI rats. The only regions of the cavity devoid of cells were associated with organized lesion borders and high AQP4 levels (marked with thin arrows). **(F)** DAPI channel (pseudo-colored in cyan) in a TMX-treated SCI rat. Thick white arrow: cell infiltration was also found within cavities of TMX-treated SCI rats, but only in limited regions where cavity walls were disorganized and expressed lower AQP4 levels. Thin white arrow: more organized lesion border were associated with higher AQP4 levels and lack of cell infiltration. **(G)** Quantitative analysis of the DAPI-labeled nuclei within the cavity (Y-axis: number of nuclei per μm^2) showed two-fold fewer nuclei in TMX-treated SCI rats (five random 10th thoracic segment sections /rat; $n =$ five rats/group). Mean $\pm$ SD; $* = p < 0.05$. **(H)** The cells within cavities included immature, radial glia-like astrocytes labeled with 3CB2, and reactive microglia labeled with Iba-1. Calibration line: 10 μm. Color image is available online at www.liebertpub.com/neu

Table 3. Translatability of TMX

Criteria for translational potential	*Our analyses*	*Results presented in*	*Conclusions*
Animal model representative of SCI in humans	Rat contusion T10		
Systemic administration	S.Q. pellets		Readily crosses the blood brain barrier; so any systemic route is possible including S.Q. pellets
Timing of therapy	Acute and Chronic	Fig. 1A and 1D	Only acute administration, starting at 2 h after SCI
Limited duration of therapy	14 and 28 days	Fig. 1A and 1D	14 days; longer than 14 days was not more effective
Dose	4mg/kg/day	Fig. 1A	Clinical dose is ~0.3-1mg/kg/day for 5 years; so 4mg/kg/day for 2 weeks should be safe
Toxicity	Liver	Methods section	No apparent toxicity
Clinically relevant improvement	BBB scores	Fig. 1A	Consistent with fore/hind limb coordination vs. failure
Mechanism of neuroprotection	Proteomics/WB/ histology	Fig. 2-6	Spared oligodendrocytes/myelin and decreased cavitation
Reproducibility			Tian et al. (2009)

SCI, spinal cord injury; T10, tenth thoracic segment; SQ, subcutaneous; BBB, Basso, Beattie, and Bresnahan locomotive rating scale; WB, Western blot.

TMX. However, multimodal therapeutic targets of TMX (estrogen receptor and non-estrogen receptor-mediated pathways) are not affected by either of the promising pharmacological interventions mentioned above, and may explain a unique neuroprotective effect of TMX, discussed below.

Proteomic analysis of TMX treatment. Given that TMX can affect many cell types in the CNS, and stimulate a plethora of signaling pathways (as described in the Introduction), we used a global proteomic analysis to shed light on the mechanisms underlying beneficial effect of TMX in SCI. The results of our proteomic analysis (summarized in Table 2) are consistent with the proteomic analyses of TMX effects in breast cancer cells, which, similar to our study, also identified stathmin, protein disulfide isomerase A3, peroxiredoxin, and GFAP as TMX targets,[55] thus validating our results. However, the initial goal of our proteomic analysis was to identify markers of cell populations affected by TMX, rather than to identify a complete list of proteins affected by TMX because of the inherent limitations of the proteomic method that generates a large number of false negatives. For example, we found that TMX significantly affected MBP, MOG and AQP4 levels when we used Western blots but not when we analyzed proteomic data. This can be explained by either the well-known lower sensitivity of the proteomic analysis versus Western blots or by the stringency of our statistical analysis. Because we used corrections for multiple comparisons, we eliminated from the analysis a large number of proteins (1118-25 = 1093 spots), in part because of the intra-group variations, which if analyzed for individual proteins, might have rendered some differences between treatments groups significant. As our proteomic analysis identified several oligodendrocytic and astrocytic proteins as being significantly affected by TMX (see Table 2), we focused our further analyses on those two cell populations, although the effect of TMX on other cell types present at the lesion site 35 days after SCI cannot be ruled out.

TMX effects on oligodendrocyte/myelin levels can explain the improvement in BBB scores. We have shown that loss of myelin levels at the lesion site in chronically injured spinal cords is correlated with BBB scores,[56] in agreement with other findings.[57] Further, we have also demonstrated that even modest increases in myelin (i.e., MOG) levels by ~12% at the lesion site lead to substantial improvements of locomotor recovery.[56] Therefore, our finding that TMX increases levels of all major myelin proteins (MBP, CNPase, MOG), and oligodendrocyte numbers by ~20% at T10 can explain the observed improvement in hind-limb motor recovery (by ~3 BBB scores).

We have previously shown that acute loss of myelin at the lesion site (~40% decrease) occurs within the first 24 h after SCI, followed by additional >40% decrease that is finalized by seven days after SCI,[56] consistent with a delayed wave of oligodendrocyte death.[58–60] Given the delayed locomotor improvement of TMX-treated SCI rats (14 days), and a lack of a TMX effect on the bladder function recovery (occurred at ~6 days), it is likely that TMX reduced the delayed loss of oligodendrocytes, and the resultant loss of myelin and axonal demyelination/dysfunction that is critically important for the functional recovery after SCI.[57] Although the effect of TMX on oligodendrocyte survival after trauma has not been studied, Lee and colleagues,[61] have shown that 17β-estradiol reduces oligodendrocyte cell death by inhibiting JNK3 activation, a pathway that is also implicated in oligodendrocyte apoptosis after SCI.[62] Given that TMX mimics the effects of 17β-estradiol on oligodendrocytes,[15] it is likely that TMX prevented delayed apoptotic death of oligodendrocytes after SCI.

Novel TMX effect on astrocytic AQP4

It has been shown that TMX decreases the activation of astrocytes in different conditions,[63] including SCI.[23] However, our data suggest that TMX did not decrease overall astrocytic activation as vimentin levels were not affected while AQP4 levels were further increased, consistent with TMX having complex effects on reactive astrocytes that can be either ER-mediated (agonistic[64] or antagonistic[16]) or non-ER-mediated.[20]

Although the role of estrogen in the regulation of AQP4 expression has not been studied, there are reports that would indicate that estradiol (presumably through the estrogen receptor-mediated pathways) can affect AQP4 levels. For example, estrogen withdrawal results in reduced AQP4 levels in rat brains.[65] However,

exogenous administration of estradiol also decreases AQP4 levels in ischemic brain.[66] Given that published findings linking AQP4 and ER are scarce and controversial and that our study is the first to report the effect of tamoxifen on AQP4 levels in injured spinal cords, it remains to be determined if TMX effects on AQP4 levels are ER- or non–ER-dependent.

We have already demonstrated that higher AQP4 levels in chronically injured spinal cords are associated with better functional recovery after SCI,[67] in agreement with an AQP4 deletion study showing that a lack of AQP4 impairs locomotor recovery in SCI mice.[68] However, the role of AQP4 increases in chronically injured spinal cords is not known. Our data indicate that AQP4 increases in TMX-treated chronically injured SCI rats were associated with the formation of a glia limitans–like organization of the cavity walls and smaller fluid-filled cavities, a novel finding. We hypothesize that increased AQP4 may facilitate specific ''stacking'' arrangement[69] of the glia limitans subtype of astrocytes,[70] which could prevent fluid accumulation and/or spreading of reactive glia (see Fig. 6H), and thus limit progressive cavitation after SCI. Interestingly, Kimura and colleagues[68] have shown that AQP4 knockout SCI mice not only recover locomotion more poorly than wild type SCI mice but also form fluid-filled cavities,[68] while wild type SCI mice never form cysts, further supporting our hypothesis that TMX-mediated AQP4 increases limit the expansion of the fluid-filled cavities.

Our data also suggest that TMX increased levels of the M23 isoform $\sim$2.5 times more than levels of the M1 AQP4 isoform. In contrast to M1, M23 isoform is capable of assembling into large and immobile orthogonal arrays of particles (OAP)[71,72] that may contribute to the specific stacking arrangement possibly through intercellular OAP interactions among glia limitans–forming astrocytes. It is also interesting that irregularly shaped, ''open'' cavities containing cells, as described in our control SCI rats, closely resembled lesions in humans SCI associated with astrocytes not expressing AQP4,[67] suggesting that more profound dysfunction of AQP4 after SCI in humans may be one of the factors contributing to the vastly poorer functional recovery than in rodent models of SCI characterized by AQP4 upregulation.

Together, our data strongly suggest that TMX delivery should last for two weeks after SCI, and that during the first week post-injury, TMX alleviates protracted death of oligodendrocyte and thus prevents debilitating demyelination, while in the second week, it limits cavitation by upregulating AQP4—all processes leading to the improved locomotor recovery of SCI rats. Therefore, we propose TMX as a promising therapeutic intervention for SCI. However, we also believe that the effect of TMX on myelin levels and its novel effect on AQP4 may also be potentially useful for the treatment of other demyelinating diseases particularly if associated with the loss of both myelin and AQP4, such as neuromyelitis optica (Devic's disease).[73]

Acknowledgments

We thank Dr. Jason Vellano for the gross morphological and histological assessments of the liver and GI tract in our experimental animals. We also thank Dr. David Konkel for critically editing the manuscript.

Author Disclosure Statement

This work was supported by Mission Connect, a program of the TIRR Foundation. No competing financial interests exist.

References

1. Amtul, Z., Wang, L., Westaway, D., and Rozmahel, R. F. (2010). Neuroprotective mechanism conferred by 17beta-estradiol on the biochemical basis of Alzheimer's disease. Neuroscience 169, 781–786.
2. Bourque, M., Dluzen, D. E., and Di, Paolo T. (2009). Neuroprotective actions of sex steroids in Parkinson's disease. Front Neuroendocrinol. 30, 142–157.
3. Garcia-Segura, L. M. and Melcangi, R. C. (2006). Steroids and glial cell function. Glia 54, 485–498.
4. Lebesgue, D., Chevaleyre, V., Zukin, R. S., and Etgen, A. M. (2009). Estradiol rescues neurons from global ischemia-induced cell death: multiple cellular pathways of neuroprotection. Steroids 74, 555–561.
5. Samantaray, S., Sribnick, E. A., Das, A., Thakore, N. P., Matzelle, D., Yu, S. P., Ray, S. K., Wei, L., and Banik, N. L. (2010). Neuroprotective efficacy of estrogen in experimental spinal cord injury in rats. Ann. N. Y. Acad. Sci. 1199, 90–94.
6. Mhyre, A. J. and Dorsa, D. M. (2006). Estrogen activates rapid signaling in the brain: role of estrogen receptor alpha and estrogen receptor beta in neurons and glia. Neuroscience 138, 851–858.
7. Hosli, E., Jurasin, K., Ruhl, W., Luthy, R., and Hosli, L. (2001). Colocalization of androgen, estrogen and cholinergic receptors on cultured astrocytes of rat central nervous system. Int. J. Dev. Neurosci. 19, 11–19.
8. Platania, P., Laureanti, F., Bellomo, M., Giuffrida, R., Giuffrida-Stella, A. M., Catania, M. V., and Sortino, M. A. (2003). Differential expression of estrogen receptors alpha and beta in the spinal cord during postnatal development: localization in glial cells. Neuroendocrinology 77, 334–340.
9. Brzozowski, A. M., Pike, A. C., Dauter, Z., Hubbard, R. E., Bonn, T., Engstrom, O., Ohman, L., Greene, G. L., Gustafsson, J. A., and Carlquist, M. (1997). Molecular basis of agonism and antagonism in the oestrogen receptor. Nature 389, 753–758.
10. Paige, L. A., Christensen, D. J., Gron, H., Norris, J. D., Gottlin, E. B., Padilla, K. M., Chang, C. Y., Ballas, L. M., Hamilton, P. T., McDonnell, D. P., and Fowlkes, D. M. (1999). Estrogen receptor (ER) modulators each induce distinct conformational changes in ER alpha and ER beta. Proc. Natl. Acad. Sci. U. S. A. 96, 3999–4004.
11. Belandia, B. and Parker, M. G. (2003). Nuclear receptors: a rendezvous for chromatin remodeling factors. Cell 114, 277–280.
12. Klinge, C. M. (2000). Estrogen receptor interaction with co-activators and co-repressors. Steroids 65, 227–251.
13. McKenna, N. J. and O'Malley, B. W. (2002). Combinatorial control of gene expression by nuclear receptors and coregulators. Cell 108, 465–474.
14. Norris, J. D., Paige, L. A., Christensen, D. J., Chang, C. Y., Huacani, M. R., Fan, D., Hamilton, P. T., Fowlkes, D. M., and McDonnell, D. P. (1999). Peptide antagonists of the human estrogen receptor. Science 285, 744–746.
15. Marin-Husstege, M., Muggironi, M., Raban, D., Skoff, R. P., and Casaccia-Bonnefil, P. (2004). Oligodendrocyte progenitor proliferation and maturation is differentially regulated by male and female sex steroid hormones. Dev. Neurosci. 26, 245–254.
16. Garcia-Segura, L. M., Cardona-Gomez, P., Naftolin, F., and Chowen, J. A. (1998). Estradiol upregulates Bcl-2 expression in adult brain neurons. Neuroreport 9, 593–597.
17. de, Medina P., Favre, G., and Poirot, M. (2004). Multiple targeting by the antitumor drug tamoxifen: a structure-activity study. Curr. Med. Chem. Anticancer Agents 4, 491–508.
18. Amrollahi, Z., Rezaei, F., Salehi, B., Modabbernia, A. H., Maroufi, A., Esfandiari, G. R., Naderi, M., Ghebleh, F., Ahmadi-Abhari, S. A., Sadeghi, M., Tabrizi, M., and Akhondzadeh, S. (2011). Double-blind, randomized, placebo-controlled 6-week study on the efficacy and safety of the tamoxifen adjunctive to lithium in acute bipolar mania. J. Affect. Disord. 129, 327–331.
19. Mao, J., Yuan, J., Wang, L., Zhang, H., Jin, X., Zhu, J., Li, H., Xu, B., and Chen, L. (2013). Tamoxifen inhibits migration of estrogen receptor-negative hepatocellular carcinoma cells by blocking the swelling-activated chloride current. J. Cell Physiol. 228, 991–1001.
20. Kimelberg, H. K. (2005). Astrocytic swelling in cerebral ischemia as a possible cause of injury and target for therapy. Glia 50, 389–397.
21. Arevalo, M. A., Diz-Chaves, Y., Santos-Galindo, M., Bellini, M. J., and Garcia-Segura, L. M. (2012). Selective oestrogen receptor modulators decrease the inflammatory response of glial cells. J. Neuroendocrinol. 24, 183–190.

22. Ismailoğlu, O., Oral, B., Görgülü, A., Sütçü, R., Demir, N. (2010). Neuroprotective effects of tamoxifen on experimental spinal cord injury in rats. J. Clin Neurosci. 17, 1306–1310.
23. Tian, D. S., Liu, J. L., Xie, M. J., Zhan, Y., Qu, W. S., Yu, Z. Y., Tang, Z. P., Pan, D. J., and Wang, W. (2009). Tamoxifen attenuates inflammatory-mediated damage and improves functional outcome after spinal cord injury in rats. J. Neurochem. 109, 1658–1667.
24. Durham-Lee, J. C., Wu, Y., Mokkapati, V. U., Paulucci-Holthauzen, A. A., and Nesic, O. (2012). Induction of angiopoietin-2 after spinal cord injury. Neuroscience 202, 454–464.
25. Kisanga, E. R., Gjerde, J., Schjott, J., Mellgren, G., and Lien, E. A. (2003). Tamoxifen administration and metabolism in nude mice and nude rats. J. Steroid Biochem. Mol. Biol. 84, 361–367.
26. Robins, H. I., Won, M., Seiferheld, W. F., Schultz, C. J., Choucair, A. K., Brachman, D. G., Demas, W. F., and Mehta, M. P. (2006). Phase 2 trial of radiation plus high-dose tamoxifen for glioblastoma multiforme: RTOG protocol BR-0021. Neuro. Oncol. 8, 47–52.
27. Greaves, P., Goonetilleke, R., Nunn, G., Topham, J., and Orton, T. (1993). Two-year carcinogenicity study of tamoxifen in Alderley Park Wistar-derived rats. Cancer Res. 53, 3919–3924.
28. Basso, D. M., Beattie, M. S., and Bresnahan, J. C. (1995). A sensitive and reliable locomotor rating scale for open field testing in rats. J. Neurotrauma 12, 1–21.
29. Pretzer, E. and Wiktorowicz, J. E. (2008). Saturation fluorescence labeling of proteins for proteomic analyses. Anal. Biochem. 374, 250–262.
30. Straub, C., Pazdrak, K., Young, T. W., Stafford, S. J., Wu, Z., Wiktorowicz, J. E., Haag, A. M., English, R. D., Soman, K. V., and Kurosky, A. (2009). Toward the Proteome of the Human Peripheral Blood Eosinophil. Proteomics. Clin. Appl. 3, 1151–1173.
31. Guptarak, J., Wanchoo, S., Durham-Lee, J., Wu, Y., Zivadinovic, D., Paulucci-Holthauzen, A., and Nesic, O. (2013). Inhibition of IL-6 signaling:Anovel therapeutic approach to treating spinal 3cord injury pain. Pain 154,1115–1128.
32. Papkoff, J., Rubinfeld, B., Schryver, B., and Polakis, P. (1996). Wnt-1 regulates free pools of catenins and stabilizes APC-catenin complexes. Mol. Cell Biol. 16, 2128–2134.
33. McMahon, S. S. and McDermott, K. W. (2002). Morphology and differentiation of radial glia in the developing rat spinal cord. J. Comp Neurol. 454, 263–271.
34. Benjamini, Y. and Hochberg, Y. (1995). Controlling the false discovery rate: a practical and powerful approach to multiple testing. J. R. Statist. Soc. B. 57, 289–300.
35. R Development Core Team R: A language and environment for statistical computing. R Foundation for Statistical Computing: Vienna, Austria.
36. Fudge, M. A., Kavaliers, M., Baird, J. P., and Ossenkopp, K. P. (2009). Tamoxifen produces conditioned taste avoidance in male rats: an analysis of microstructural licking patterns and taste reactivity. Horm. Behav. 56, 322–331.
37. Gray, J. M., Schrock, S., and Bishop, M. (1993). Estrogens and antiestrogens: actions and interactions with fluphenazine on food intake and body weight in rats. Am. J. Physiol. 264, R1214–R1218.
38. Lopez, M., Lelliott, C. J., Tovar, S., Kimber, W., Gallego, R., Virtue, S., Blount, M., Vazquez, M. J., Finer, N., Powles, T. J., O'Rahilly, S., Saha, A. K., Dieguez, C., and Vidal-Puig, A. J. (2006). Tamoxifen-induced anorexia is associated with fatty acid synthase inhibition in the ventromedial nucleus of the hypothalamus and accumulation of malonyl-CoA. Diabetes 55, 1327–1336.
39. Wade, G. N. and Heller, H. W. (1993). Tamoxifen mimics the effects of estradiol on food intake, body weight, and body composition in rats. Am. J. Physiol 264, R1219–R1223.
40. Kasama-Yoshida, H., Tohyama, Y., Kurihara, T., Sakuma, M., Kojima, H., and Tamai, Y. (1997). A comparative study of 2′,3′-cyclic-nucleotide 3′-phosphodiesterase in vertebrates: cDNA cloning and amino acid sequences for chicken and bullfrog enzymes. J. Neurochem. 69, 1335–1342.
41. Liu, A., Stadelmann, C., Moscarello, M., Bruck, W., Sobel, A., Mastronardi, F. G., and Casaccia-Bonnefil, P. (2005). Expression of stathmin, a developmentally controlled cytoskeleton-regulating molecule, in demyelinating disorders. J. Neurosci. 25, 737–747.
42. Nielsen, J. A., Maric, D., Lau, P., Barker, J. L., and Hudson, L. D. (2006). Identification of a novel oligodendrocyte cell adhesion protein using gene expression profiling. J. Neurosci. 26, 9881–9891.
43. Mondal, S., Dirks, P., and Rutka, J. T. (2010). Immunolocalization of fascin, an actin-bundling protein and glial fibrillary acidic protein in human astrocytoma cells. Brain Pathol. 20, 190–199.
44. Yamasaki, M., Yamada, K., Furuya, S., Mitoma, J., Hirabayashi, Y., and Watanabe, M. (2001). 3-Phosphoglycerate dehydrogenase, a key enzyme for l-serine biosynthesis, is preferentially expressed in the radial glia/astrocyte lineage and olfactory ensheathing glia in the mouse brain. J. Neurosci. 21, 7691–7704.
45. Berg, R. W., Chen, M. T., Huang, H. C., Hsiao, M. C., and Cheng, H. (2009). A method for unit recording in the lumbar spinal cord during locomotion of the conscious adult rat. J. Neurosci. Methods 182, 49–54.
46. Falgairolle, M., de, Seze M., Juvin, L., Morin, D., and Cazalets, J. R. (2006). Coordinated network functioning in the spinal cord: an evolutionary perspective. J. Physiol. Paris 100, 304–316.
47. Fuss, B., Mallon, B., Phan, T., Ohlemeyer, C., Kirchhoff, F., Nishiyama, A., and Macklin, W. B. (2000). Purification and analysis of in vivo-differentiated oligodendrocytes expressing the green fluorescent protein. Dev. Biol. 218, 259–274.
48. Nesic, O., Lee, J., Ye, Z., Unabia, G. C., Rafati, D., Hulsebosch, C. E., and Perez-Polo, J. R. (2006). Acute and chronic changes in aquaporin 4 expression after spinal cord injury. Neuroscience 143, 779–792.
49. Tator, C. H., Hashimoto, R., Raich, A., Norvell, D., Fehlings, M. G., Harrop, J. S., Guest, J., Aarabi, B., and Grossman, R. G. (2012). Translational potential of preclinical trials of neuroprotection through pharmacotherapy for spinal cord injury. J. Neurosurg. Spine 17, 157–229.
50. Guest, J., Harrop, J. S., Aarabi, B., Grossman, R. G., Fawcett, J. W., Fehlings, M. G., and Tator, C. H. (2012). Optimization of the decision-making process for the selection of therapeutics to undergo clinical testing for spinal cord injury in the North American Clinical Trials Network. J. Neurosurg. Spine 17, 94–101.
51. O'Brian, C. A., Liskamp, R. M., Solomon, D. H., and Weinstein, I. B. (1985). Inhibition of protein kinase C by tamoxifen. Cancer Res. 45, 2462–2465.
52. O'Brian, C. A., Housey, G. M., and Weinstein, I. B. (1988). Specific and direct binding of protein kinase C to an immobilized tamoxifen analogue. Cancer Res. 48, 3626–3629.
53. Zarate, C. A., Jr., Singh, J. B., Carlson, P. J., Quiroz, J., Jolkovsky, L., Luckenbaugh, D. A., and Manji, H. K. (2007). Efficacy of a protein kinase C inhibitor (tamoxifen) in the treatment of acute mania: a pilot study. Bipolar Disord. 9, 561–570.
54. Kisanga, E. R., Gjerde, J., Guerrieri-Gonzaga, A., Pigatto, F., Pesci-Feltri, A., Robertson, C., Serrano, D., Pelosi, G., Decensi, A., and Lien, E. A. (2004). Tamoxifen and metabolite concentrations in serum and breast cancer tissue during three dose regimens in a randomized preoperative trial. Clin. Cancer Res. 10, 2336–2343.
55. Lochab, S., Pal, P., Kanaujiya, J. K., Tripathi, S. B., Kapoor, I., Bhatt, M. L., Sanyal, S., Behre, G., and Trivedi, A. K. (2012). Proteomic identification of E6AP as a molecular target of tamoxifen in MCF7 cells. Proteomics 12, 1363–1377.
56. Durham-Lee, J. C., Mokkapati, V. U., Johnson, K. M., and Nesic, O. (2011). Amiloride improves locomotor recovery after spinal cord injury. J. Neurotrauma 28, 1319–1326.
57. Cao, Q., He, Q., Wang, Y., Cheng, X., Howard, R. M., Zhang, Y., DeVries, W. H., Shields, C. B., Magnuson, D. S., Xu, X. M., Kim, D. H., and Whittemore, S. R. (2010). Transplantation of ciliary neurotrophic factor-expressing adult oligodendrocyte precursor cells promotes remyelination and functional recovery after spinal cord injury. J. Neurosci. 30, 2989–3001.
58. Crowe, M. J., Bresnahan, J. C., Shuman, S. L., Masters, J. N., and Beattie, M. S. (1997). Apoptosis and delayed degeneration after spinal cord injury in rats and monkeys. Nat. Med. 3, 73–76.
59. Liu, X. Z., Xu, X. M., Hu, R., Du, C., Zhang, S. X., McDonald, J. W., Dong, H. X., Wu, Y. J., Fan, G. S., Jacquin, M. F., Hsu, C. Y., and Choi, D. W. (1997). Neuronal and glial apoptosis after traumatic spinal cord injury. J. Neurosci. 17, 5395–5406.
60. Shuman, S. L., Bresnahan, J. C., and Beattie, M. S. (1997). Apoptosis of microglia and oligodendrocytes after spinal cord contusion in rats. J. Neurosci. Res. 50, 798–808.
61. Lee, J. Y., Choi, S. Y., Oh, T. H., and Yune, T. Y. (2012). 17beta-Estradiol inhibits apoptotic cell death of oligodendrocytes by inhibiting RhoA-JNK3 activation after spinal cord injury. Endocrinology 153, 3815–3827.

62. Li, Q. M., Tep, C., Yune, T. Y., Zhou, X. Z., Uchida, T., Lu, K. P., and Yoon, S. O. (2007). Opposite regulation of oligodendrocyte apoptosis by JNK3 and Pin1 after spinal cord injury. J. Neurosci. 27, 8395–8404.
63. Arevalo, M. A., Santos-Galindo, M., Lagunas, N., Azcoitia, I., and Garcia-Segura, L. M. (2011). Selective estrogen receptor modulators as brain therapeutic agents. J. Mol. Endocrinol. 46, R1–R9.
64. Cerciat, M., Unkila, M., Garcia-Segura, L. M., and Arevalo, M. A. (2010). Selective estrogen receptor modulators decrease the production of interleukin-6 and interferon-gamma-inducible protein-10 by astrocytes exposed to inflammatory challenge in vitro. Glia 58, 93–102.
65. Suda, S., Segi-Nishida, E., Newton, S.S., Duman, R.S. (2008). A postpartum model in rat: behavioral and gene expression changes induced by ovarian steroid deprivation. Biol. Psychiatry 64, 311–319.
66. Rutkowsky, J.M., Wallace, B.K., Wise, P.M., O'Donnell, M.E. (2011). Effects of estradiol on ischemic factor-induced astrocyte swelling and AQP4 protein abundance. Am. J. Physiol. Cell Physiol. 301, C204–12.
67. Nesic, O., Guest, J. D., Zivadinovic, D., Narayana, P. A., Herrera, J. J., Grill, R. J., Mokkapati, V. U., Gelman, B. B., and Lee, J. (2010). Aquaporins in spinal cord injury: the janus face of aquaporin 4. Neuroscience 168, 1019–1035.
68. Kimura, A., Hsu, M., Seldin, M., Verkman, A. S., Scharfman, H. E., and Binder, D. K. (2010). Protective role of aquaporin-4 water channels after contusion spinal cord injury. Ann. Neurol. 67, 794–801.
69. Nielsen, S., Nagelhus, E. A., Amiry-Moghaddam, M., Bourque, C., Agre, P., and Ottersen, O. P. (1997). Specialized membrane domains for water transport in glial cells: high-resolution immunogold cytochemistry of aquaporin-4 in rat brain. J. Neurosci. 17, 171–180.
70. Holen, T. (2011). The ultrastructure of lamellar stack astrocytes. Glia 59, 1075–1083.
71. Crane, J. M., Bennett, J. L., and Verkman, A. S. (2009). Live cell analysis of aquaporin-4 m1/m23 interactions and regulated orthogonal array assembly in glial cells. J. Biol. Chem. 284, 35850–35860.
72. Sorbo, J. G., Moe, S. E., Ottersen, O. P., and Holen, T. (2008). The molecular composition of square arrays. Biochemistry 47, 2631–2637.
73. Ratelade, J. and Verkman, A. S. (2012). Neuromyelitis optica: aquaporin-4 based pathogenesis mechanisms and new therapies. Int. J. Biochem. Cell Biol. 44, 1519–1530.

Address correspondence to:
Olivera Nesic, PhD
Department of Medical Education Texas Tech University
Paul L. Foster School of Medicine
El Paso, TX 79905

E-mail: olivera.nesic-taylor@ttuhsc.edu